

**Rat bone marrow stromal cells-seeded porous
gelatin/tricalcium phosphate/oligomeric proanthocyanidins
composite scaffold for bone repair**

Journal:	<i>Journal of Tissue Engineering and Regenerative Medicine</i>
Manuscript ID:	TERM-10-0308.R1
Wiley - Manuscript type:	Research Article
Date Submitted by the Author:	n/a
Complete List of Authors:	Chen, Kuo-Yu; National Yunlin University of Science and Technology, Department of Chemical and Materials Engineering Chung, Chia-Mei; Central Taiwan University of Science and Technology Bau, Da-Tian; China Medical University and Hospital Chen, Yueh-Sheng; China Medical University Yao, Chun-Hsu; China Medical University
Keywords:	bone tissue engineering, porous, bone marrow stromal cells, oligomeric proanthocyanidins, gelatin, tricalcium phosphate

SCHOLARONE™
Manuscripts

1
2
3
4
5
6
7
8
9
10
11
12
13
14
15
16
17
18
19
20
21
22
23
24
25
26
27
28
29
30
31
32
33
34
35
36
37
38
39
40
41
42
43
44
45
46
47
48
49
50
51
52
53
54
55
56
57
58
59
60

Rat bone marrow stromal cells-seeded porous gelatin/tricalcium phosphate/oligomeric proanthocyanidins composite scaffold for bone repair

Short title: BMSCs-seeded porous gelatin composite for bone repair

Kuo-Yu Chen¹, Chia-Mei Chung², Da-Tian Bau³, Yueh-Sheng Chen^{4,5,†}
and Chun-Hsu Yao^{4,5*,†}

¹Department of Chemical and Materials Engineering, National Yunlin
University of Science and Technology, Yunlin, Taiwan

²Institute of Biomedical Engineering and Material Science, Central Taiwan
University of Science and Technology, Taichung, Taiwan

³Terry Fox Cancer Research Lab, China Medical University and Hospital,
Taichung, Taiwan

⁴Department of Biomedical Imaging and Radiological Science, China
Medical University, Taichung, Taiwan

⁵School of Chinese Medicine, China Medical University, Taichung, Taiwan

**Correspondence to: C.H. Yao, Department of Biomedical Imaging and
Radiological Science, China Medical University, Taichung, 40402, Taiwan.*

Telephone Number: +886-4-22053366 ext. 7806;

FAX Number: +886-4-2207-6976; E-mail: chyao@mail.cmu.edu.tw

† These authors contributed equally to this work.

Abstract

Repair of bone defects remains a major challenge in orthopaedic surgery. Bone tissue engineering is an attractive approach for treating bone loss in various shapes and amounts. The aim of this study was to prepare and evaluate the feasibility of a porous scaffold (GTP) seeded with bone marrow stromal cells (BMSCs) as a bone substitute. GTP scaffolds composed of oligomeric proanthocyanidins cross-linked gelatin and β -tricalcium phosphate were made porous using a salt-leaching method. The physicochemical properties of the scaffold were evaluated to determine the optimal salt/composite weight ratio. The results indicated that GTP scaffold had a favorable macroporous structure and higher porosity when the weight ratio of salt to composite was 4:1. Cytotoxic tests demonstrated that the extracts from GTP scaffolds promoted the proliferation of BMSCs. Rat BMSCs were seeded on a porous GTP scaffold and cultured in a spinner flask. After two weeks of culture, the cells exhibited good affinity toward the surfaces of the pores in the scaffold. Moreover, this study explored the biological response of rat calvarial bone to the scaffold to evaluate its potential in bone tissue engineering. Bone defects were filled with BMSCs-seeded GTP scaffold and acellular GTP scaffold. After eight weeks, the scaffold induced new bone formation at a bone defect with a diameter of 7 mm, as was confirmed by X-ray microradiography and histology. The BMSC-seeded scaffold induced more new bone formation than did an acellular scaffold. These observations suggest that the BMSCs-seeded GTP scaffold can promote the regeneration of defective bone tissue.

Keywords bone tissue engineering; porous; bone marrow stromal cells; oligomeric proanthocyanidins; gelatin; tricalcium phosphate

1. Introduction

Bone tissue engineering is an emerging approach for the effective repair of bone defects with various shapes and sizes, which may be caused by trauma, inflammation, tumor resection or skeletal abnormalities. Successful regeneration of damaged tissue through tissue engineering depends on a suitable source of cells, appropriate culture conditions and a biocompatible scaffold. An ideal scaffold for use as a temporal template for the *in vitro* and *in vivo* formation of bone tissues should promote the migration of bone cells toward, and then inside, those tissues to replace the scaffold.

Tricalcium phosphate ($\text{Ca}_3(\text{PO}_4)_2$), a synthetic bone-promoting biomaterial, has been widely applied and investigated as a biodegradable bone replacement (Ogose *et al.*, 2006). It can strengthen the osteoconductive characteristics of scaffolds, but it is difficult to keep within the reconstructed area and it lacks structural stability. Gelatin, a partially denatured derivative of collagen, can bind tricalcium phosphate to form composites with high biocompatibility, adhesiveness and plasticity (Bigi *et al.*, 2004). Gelatin has been extensively used as a scaffold in bone tissue engineering owing its cytocompatibility (Kim *et al.*, 2005a).

Bone marrow stromal cells (BMSCs) are promising for the restoration of bone defects because of their relative ease of procurement, large expansion and strong osteogenic differentiation capabilities (Bruder *et al.*, 1998a). BMSCs have been demonstrated to be effective in healing bone defects in various animal models (Kim *et al.*, 2005c; Kon *et al.*, 2000). The composition of scaffolds can substantially affect the proliferation and osteogenic differentiation of BMSCs (Takahashi *et al.*, 2005). In recent years, a few researchers have explored the combination of BMSCs with gelatin-based scaffolds in bone tissue engineering (Bernhardt *et al.*, 2009; Tabata *et al.*, 2000;

1
2
3
4 Takahashi *et al.*, 2005; Zhao *et al.*, 2006). However, gelatin is easily resorbable *in vivo*.
5
6 Various synthetic cross-linkers have been employed to cross-link gelatin and improve
7
8 the mechanical properties of gelatin-based composites (Sung *et al.*, 1999). Most of these
9
10 synthetic cross-linkers are, however, highly cytotoxic, reducing the biocompatibility of
11
12 bioprotheses (Lin *et al.*, 1998). Recently, a few investigators have shown that
13
14 oligomeric proanthocyanidins (OPCs), naturally occurring cross-linkers, can fix
15
16 biologic tissues and biomaterials effectively without cytotoxicity (Han *et al.*, 2003; Kim
17
18
19
20
21 *et al.*, 2005b; Zhai *et al.*, 2006).

22
23 In the authors' recent study, OPCs were used to cross-link a gelatin/ β -tricalcium
24
25 phosphate mixture (Chen *et al.*, 2008). An evaluation of cytotoxicity revealed that the
26
27 extract of the composite not only was nontoxic, but also promoted the proliferation of
28
29 MG-63 cells. The residual gelatin and calcium released from the composite were
30
31 supposed to be nutritious for the growth of the bone cells (Liu *et al.*, 2003). Furthermore,
32
33 the results concerning the biological response of rabbit calvarial bone to the composite
34
35 demonstrated progressive growth of new bone into the calvarial bone defect (Chen *et al.*,
36
37 2009). The biodegradability and biocompatibility of the composite make it promising in
38
39 the clinical repair of large bone defects. However, the composite has a dense
40
41 morphology after freeze-drying. The dense surface does not allow cells to penetrate into
42
43 the interior areas when the cell suspension is seeded on the scaffold. Furthermore, the
44
45 dense structure detrimentally affects cell in-growth during *in vitro* cell culture.
46
47
48
49

50
51 Successful bone tissue engineering depends on a highly porous and interconnected
52
53 pore structure to enable the passage of oxygen and nutrients to the attached cells inside
54
55 the scaffold, and to facilitate the transfer of metabolic waste out of it. Moreover, a
56
57 macroporous design promotes the in-growth of both new bone tissue and blood vessel
58
59
60

1
2
3
4 following implantation. Porous three-dimensional scaffolds can be manufactured by
5
6 various approaches, including the use of porogens, gas forming, phase separation,
7
8 three-dimensional printing and rapid prototyping. Several researchers have used
9
10 salt-leaching method to prepare porous gelatin-based scaffolds in aqueous solution. For
11
12 instance, Lee *et al.* (2005) applied sodium chloride crystals as a porogen to prepare
13
14 porous gelatin scaffolds with a uniformly distributed and interconnected pore structure.
15
16 Their porosity and pore size were established to be controllable by varying the particle
17
18 size and salt content.
19
20
21
22

23 The *in vivo* formation of bone using gelatin-based scaffold with a combination of
24
25 BMSCs and dynamic culture before implantation has not yet been reported upon. In this
26
27 study, biodegradable composites based on gelatin, β -tricalcium phosphate and OPCs
28
29 were prepared and a salt-leaching approach was used to make macroporous GTP
30
31 scaffolds for bone tissue engineering. The effects of salt content on the scaffold
32
33 characteristics were elucidated. Rat BMSCs were harvested, expanded and seeded onto
34
35 the porous GTP scaffolds. Each cell-seeded scaffold was cultured in osteogenic
36
37 induction medium and then incubated in a spinner flask. It was then used to fill the
38
39 defect cavity of a rat to evaluate its compatibility with tissue and effectiveness in bone
40
41 repair *in vivo*. This evaluation involved serial post-operative gross examination,
42
43 radiographic measurement and histological analysis.
44
45
46
47
48
49
50
51
52
53
54
55
56
57
58
59
60

2. Materials and methods

2.1. Preparation of porous GTP scaffolds

A homogeneous 18 wt% gelatin solution was obtained by dissolving porcine gelatin powder (Bloom number 300, Sigma-Aldrich, St. Louis, MO, USA) in deionized water at 75°C in a water bath. β -Tricalcium phosphate ceramic particles (Merck, Darmstadt, Germany) with grain sizes of 200–300 μm were mixed with the gelatin solution at 75°C. The weight ratio of tricalcium phosphate to gelatin was 1:1. As the gelatin/ β -tricalcium phosphate mixture was cooled down to 40°C, various amounts of sieved sodium chloride particles of size 420–590 μm were separately added to the mixture as a porogen and mixed to homogeneity. The sodium chloride particles were dried in an oven at 170°C for 4 h before use. A 10 wt% OPCs solution (Compson Trading Co., Taichung, Taiwan) was then added to induce a cross-linking reaction at a constant temperature. Consequently, the weight ratios of salt particulates to gelatin/ β -tricalcium phosphate/OPCs composites were 3:1, 4:1 and 5:1, respectively. After 20 min of vigorous stirring, the mixtures became increasingly viscous. They were poured into plastic dishes, allowed to solidify in a refrigerator at 4°C for 24 h and frozen at –80°C for a further 24 h. The solidified composites were cut and shaped into cylindrical specimens of a particular size. The salt was caused to leach out completely by immersing the composites in deionized water for 24 h. During this period, the water was changed three times. Finally, these samples were frozen at –80°C for 24 h and lyophilized in a freeze dryer for another 24 h to make porous GTP scaffolds. The dried scaffolds were cylindrical with a diameter of 7 mm and a thickness of 5 mm. Before

1
2
3
4 they were used in the experiment, all samples were sterilized under gamma irradiation at
5
6
7 10 kGy.
8
9

10 11 **2.2. Morphologies of the scaffolds**

12
13
14 The cross-sectional morphology of scaffold was investigated under a Hitachi (Japan)
15
16 S-3000N scanning electron microscope (SEM) to determine the structure and pore size.
17
18 The test sample was frozen and dried following the aforementioned procedure. The
19
20 dried sample was immediately sputter-coated with an ultrathin layer of gold for further
21
22 SEM observation. The average pore size in the cross-section was evaluated by making
23
24 measurements of the images of the pores in the SEM micrographs.
25
26
27
28
29

30 31 **2.3. Evaluating porosity**

32
33 The porosity (average void volume) of the scaffold was determined using the
34
35 Archimedes principle. The exterior volume (V_s) of each sample was measured using a
36
37 Vernier caliper. The sample was then cut into pieces and immersed in a pycnometer that
38
39 contained deionized water. The actual volume (V_m) of the sample was calculated as V_m
40
41 $= (W_w - W_0) - (W_t - W_p)$, where W_w is the total weight of the water and the pycnometer;
42
43 W_0 is the weight of the dry pycnometer; W_t is the total weight of the water, the
44
45 pycnometer and the sample fragments and W_p is the total weight of the dry pycnometer
46
47 and dry sample fragments.
48
49
50

51
52 The porosity was determined using the formula, Porosity (%) = $(V_s - V_m)/V_s \times 100$
53
54 (%). The values are given as mean \pm standard deviation ($n = 6$).
55
56
57
58
59
60

2.4. Evaluation of the cross-linking index

A ninhydrin (2,2-dihydroxy-1,3-indanedione) assay was employed to determine the amount of free amino groups in each sample. The test sample was ground, swelled in deionized water and heated with a ninhydrin solution at 100°C for 20 min. After the test solution was cooled to 25°C and diluted in 50% isopropyl alcohol, the optical absorbance of the solution was recorded using a spectrophotometer (Spectronic Unicam Genesys™ 10, New York, NY, USA) at 570 nm and gelatin at various known concentrations as a standard. The amount of free amino groups in the test sample before (C_i) and after (C_f) cross-linking was proportional to the optical absorbance of the solution. The cross-linking index was calculated as cross-linking index (%) = $(C_i - C_f)/C_i \times 100$ (%). The values are presented as mean \pm standard deviation ($n = 6$).

2.5. Measurement of swelling ratio

The swelling behavior of scaffolds was examined by immersing them in 20 ml of PBS. After soaking for 3, 6, 12, 24, 48, 72 and 96 h at 37°C, the swollen sample was taken out, gently blotted using filter paper to remove surface liquid and immediately weighed (W_{wet}). The swollen sample was then frozen, dried (following the aforementioned procedure) and weighed (W_{dry}). The swelling ratio (ΔW (%)) of each sample at each time point was calculated according to the formula, ΔW (%) = $(W_{wet} - W_{dry})/W_{dry} \times 100$ (%). Measurements were made of four specimens of each sample.

2.6. Determination of *in vitro* degradation rate

To measure the rate of hydrolytic degradation of the scaffold, it was frozen, dried (following the above procedures) and weighed (W_0). After soaking in 20 ml of

1
2
3
4 deionized water for 1, 4, 7, 14, 28 and 42 days at 37°C, the samples were retrieved from
5
6 the deionized water, frozen, dried (following the aforementioned procedure) and
7
8 weighed (W_t). The weight loss percentage (ΔW (%)) was then calculated according to
9
10 the formula, ΔW (%) = $(W_0 - W_t)/W_0 \times 100$ (%). The rate of degradation of each
11
12 sample was then determined by the relationship between its weight loss percentage and
13
14 its soaking time. At each time point, determinations were made for four samples.
15
16
17
18
19

20 21 **2.7. Isolation of BMSCs and cell culture**

22
23 Rat BMSCs cultures were prepared according to the procedure as described previously
24
25 by van den Dolder *et al.* (2003) with only minor modification. BMSCs were obtained
26
27 from femurs of 4–6 week old Sprague-Dawley rats (which were purchased from the
28
29 National Laboratory Animal Center, Taiwan). Before the beginning of the study, the
30
31 ethical committee for animal experiments at the Central Taiwan University of Science
32
33 and Technology, Taichung, Taiwan, approved the protocols. Rats were anaesthetized
34
35 intramuscularly with Zoletil 50 (Virbac, France) and 2% Rompun solution (Bayer,
36
37 Germany) (1:2 ratio, 1 ml/kg) in an aseptic animal operation room. The femurs were
38
39 removed and dissected without adherent soft tissue. The distal ends of the bones were
40
41 then cut open with sterile scissors, and the medullary cavities were flushed through the
42
43 shaft using a syringe containing Dulbecco's modified Eagle medium (DMEM; Gibco,
44
45 Grand Island, NY, USA) supplemented with 10% fetal bovine serum (Gibco) and 1%
46
47 penicillin/streptomycin (Gibco). A suspension of BMSCs was obtained by repeated
48
49 aspiration of the cell preparation through a needle. Cells were plated in a 75 cm² cell
50
51 culture flask (Costar, Cambridge, MA, USA) and incubated at 37°C under 5% CO₂. The
52
53 culture medium was refreshed every 2 days. The adherent cells were allowed to reach
54
55
56
57
58
59
60

1
2
3
4 ~80% confluence. The cells were passaged in the culture and cells at their second to
5
6
7 third passage were used in all the experiments.
8
9

10 11 **2.8. Preparation of extracts from GTP scaffolds**

12
13
14 Each sterilized GTP scaffold sample was placed in a sterilized tube filled with 20 ml of
15
16 aseptic deionized water. After they had been soaked for 1, 4, 7, 14, 28 and 42 days at
17
18 37°C, the extracts were collected for cell culture examination.
19
20

21 22 23 **2.9. Cell proliferation**

24
25
26 Rat BMSCs were employed to evaluate the cytotoxicity of the extracts from GTP
27
28 scaffolds. After 100 μl of 5×10^4 cells/ml of cultured BMSCs was seeded in the
29
30 individual wells of a 96-well tissue culture plate and incubated for 24 h, the culture
31
32 medium was replaced with a mixture of a new culture medium and the solution to be
33
34 evaluated in a volume ratio of 1:1 (Vrouwenvelder *et al.*, 1992). In the control group,
35
36 PBS was mixed with the culture medium in a ratio of 1:1 for cell cultures. After the
37
38 cells were cultured for 2 days, their proliferation was determined by
39
40 3-(4,5-dimethylthiazol-2-yl)-2,5-diphenyl tetrazolium bromide (MTT; USB, Amersham
41
42 Life Science, Cleveland, OH, USA) assay.
43
44
45
46
47

48 After 2 days of culture, the medium was replaced with 10 μl /well of MTT solution
49
50 (5 mg/ml) and 100 μl /well of culture medium and incubated at 37°C for 4 h to enable
51
52 the formation of insoluble dark-blue formazan crystals. The solution was then removed
53
54 and 100 μl /well of acidic isopropyl alcohol (0.04 M HCl in isopropyl alcohol) was
55
56 added to all wells thorough mixing dissolved the crystals. After a few minutes at room
57
58 temperature, the optical density was measured using an ELISA reader (uQuant; Bio-Tek
59
60

1
2
3
4 Instruments Inc., Sunnyvale, CA, USA) at a wavelength of 570 nm with a reference
5
6 wavelength of 650 nm. The number of viable cells in each well was calculated by
7
8 transforming the optical density values of the MTT assay into numbers of cells/well
9
10 based on a standard curve.
11
12

13 14 15 16 **2.10. Rat BMSCs dynamically cultured with the GTP scaffold** 17

18
19 A spinner flask was employed to perform the three-dimensional culture of rat BMSCs in
20
21 a CO₂ incubator. 500 µl of 2 × 10⁶ cells/ml of cultured BMSCs was loaded onto the
22
23 sterilized GTP scaffold and allowed to infiltrate into it. After 5 ml of DMEM
24
25 supplemented with 10% fetal bovine serum, 1% penicillin/streptomycin, 50 µg/ml
26
27 L-ascorbic acid (Sigma-Aldrich), 10 mM β-glycerophosphate (Sigma-Aldrich) and 10⁻⁸
28
29 M dexamethasone (Sigma-Aldrich) had been added, the cell-seeded scaffold was
30
31 cultured at 37°C in a 5% CO₂ atmosphere for 1 day. **Immediately following incubation,**
32
33 **the seeded scaffold was placed in a spinner flask with the side arm caps loosened to**
34
35 **permit gas exchange. The flasks was filled with 120 ml of osteogenic medium and**
36
37 **stirred with a magnetic bar at 70 rpm for 10 h, and then at 50 rpm for 2 weeks.** The
38
39 apparatus was placed at 37°C in a humidified incubator containing 5% CO₂. The
40
41 medium was replaced every 3 days.
42
43
44
45
46

47
48 To make morphological observations, each sample was washed three times with
49
50 PBS to remove the non-attached cells. The adherent cells were then fixed using 2 vol%
51
52 glutaraldehyde (Acros, Geel, Belgium) in 0.1 M sodium cacodylate buffer, pH 7.4. After
53
54 48 h, the sample was washed with PBS, dehydrated through a series of graded ethanol
55
56 solutions and then dried in a critical point drier. The dry sample was immediately
57
58 sputtered with gold and viewed under an SEM.
59
60

2.11. Biological response of rat calvarial bone

Adult Sprague-Dawley rats weighing 300–350 g were used for experimental cranial implantation. All animals were anaesthetized by intramuscular injections of a combination of Zoletil 50 and 2% Rompun solution (1:2 ratio, 1 ml/kg). The head of each rat was shaved, sterilized with 10% povidone-iodine solution (Chou Jen Pharmaceutical Co., Nantou, Taiwan) and prepared for surgery, which was conducted in an aseptic animal operation room. The cranial surface was exposed by a midline incision and the overlying pericranium was then cut. A microdrill was used to form two circular defects of the parietal bone in each rat skull, each with a diameter of 7 mm. Each defect cavity was randomly filled with the BMSCs-seeded GTP scaffold or the GTP scaffold without BMSCs. Each scaffold sample was easily molded to the calvarial bone defect and did not require any fixation.

Anesthetized animals were sacrificed by administering an overdose of sodium pentobarbital. The implanted scaffolds were then harvested at 4 or 8 weeks after implantation. **Craniectomy sites with 2–3 mm of contiguous bone were removed from each skull to evaluate the ossification process not only within the applied scaffold but also in the defect located between the scaffold and the native bones.** In week 4, cells were visualized under an SEM. Each sample was fixed in 10 wt% neutral-buffered formalin solution (Merck, Whitehouse Station, NJ, USA) for 48 h, washed with PBS and dehydrated using a gradation series of ethanol: distilled water solutions. The samples were then critically point-dried, coated with gold and imaged using a Hitachi SEM. Eight weeks after implantation, bone defect repair was radiographically and histologically evaluated. Specimens were fixed with 10% phosphate-buffered formalin solution for 24 h before being analyzed radiographically using an X-ray machine.

1
2
3
4
5 For histological analysis, specimens were washed twice with PBS, fixed in 10 wt%
6 neutral-buffered formalin solution, dehydrated in a graded series of increasing
7 concentrations of ethanol, immersed in xylene and embedded in paraffin wax (Merck,
8 Whitehouse Station, NJ, USA). They were then sectioned to 10 μm thickness. Sections
9 were stained with hematoxylin and eosin (H&E; Sigma-Aldrich) to view histologically
10 bone formation at the defect under an inverted optical microscope (Axiovert 25; Carl
11 Zeiss Inc., Göttingen, Germany). Markers of osteoblast function and matrix
12 mineralization were examined by alkaline phosphatase (ALP) staining and von Kossa
13 staining, respectively. In ALP staining, sample was stained using naphthol AS-BI
14 alkaline solution (Sigma-Aldrich), following the manufacturer's instructions. For von
15 Kossa staining, sample was stained for 30 min using 5% silver nitrate (Union Chemical
16 Works Ltd., Hsinchu, Taiwan) in the dark at room temperature. The sample was rinsed
17 twice with deionized water. After it was air-dried, the sample was exposed to ultraviolet
18 light for 1 h until the color was fully developed. Then it was immersed in 5% sodium
19 thiosulfate (Union Chemical Works Ltd.) for 2 min. Finally, nodular structures were
20 visualized by counterstaining with 0.1% nuclear fast red (Sigma-Aldrich) dissolved in
21 5% aluminum sulfate (JT Baker, Phillipsburg, NJ, USA) for 5 min. After the sample was
22 washed twice with deionized water, the newly formed bone nodules were observed
23 under an optical microscope. By this method, calcium salts were stained dark
24 brown/black.

2.12. Statistical analysis

25
26
27
28 All quantitative data were presented as mean \pm standard derivation. Statistical analysis
29 was conducted using one-way analysis of variance followed by *post hoc* Fisher's LSD
30
31
32
33
34
35
36
37
38
39
40
41
42
43
44
45
46
47
48
49
50

multiple comparison test. A difference was deemed significant at $p < 0.05$.

For Peer Review

3. Results

3.1. Morphologies of the GTP scaffolds

The macroporous structure of the GTP scaffold was not achieved when the weight ratio of salt particulates to composite was below 3:1. Therefore, the salt/composite weight ratio was at least 3:1 in this study. Figure 1 presents SEM images of the cross-sectional GTP scaffolds that were prepared by salt-leaching using various concentrations of sodium chloride. As observed, the concentration of sodium chloride particles significantly influenced the pore structure of the scaffolds. A three-dimensionally interconnected structure was formed when the salt/composite weight ratio exceeded 4:1. However, the distribution of the pores in the scaffold was disordered when the salt/composite weight ratio was 5:1. The pores also had random sizes, perhaps because of the aggregation of sodium chloride particles during the preparation of the scaffold. In contrast, the pores were uniformly distributed when the salt/composite weight ratio was 4:1. The pore size was in the range 400-550 μm , which is close to the size of the sodium chloride particles used herein. This result revealed that the size of pores in the GTP scaffold was governed by the salt particles. Macropores in the scaffold were formed in the spaces that had been previously occupied by the salt particles. Additionally, numerous micropores are present on the macroporous walls, which were formed during freeze-drying.

3.2. Determination of porosity

The porosities of the GTP scaffolds with salt/composite weight ratios of 4:1 and 5:1 were determined to be around $73.4 \pm 0.3\%$ and $73.5 \pm 1.0\%$, respectively, which significantly exceeded those of 3:1 ($66.7 \pm 1.1\%$) ($p < 0.05$).

3.3. Effect of salt/composite weight ratio on the cross-linking index of the GTP scaffold

In this investigation, the gelatin/tricalcium phosphate mixtures with various amounts of salt were cross-linked with OPCs at a concentration of 10 wt%. The cross-linking indexes of the GTP scaffolds with salt/composite weight ratios of 3:1, 4:1 and 5:1 were $32.5 \pm 1.4\%$, $31.2 \pm 0.8\%$ and $31.1 \pm 3.0\%$, respectively, which exhibit no statistically significant difference ($p > 0.05$), suggesting that the salt did not influence the cross-linking reaction between gelatin and OPCs.

3.4. Measuring swelling ratio

Figure 2A plots the swelling ratios of the GTP scaffolds with various salt/composite weight ratios. As observed, the GTP scaffolds in PBS began to swell rapidly in 6 h but thereafter exhibited swelling at a significantly reduced rate. Additionally, the figure revealed that the swelling ratio of the scaffolds depended on the porosity, one increasing with the other.

3.5. Determination of *in vitro* degradation rate

In vitro hydrolytic degradation of the cross-linked GTP scaffolds with different salt/composite weight ratios continued for 42 days (Figure 2B). No remarkable difference among the degradations of these samples was observed, indicating that the amount of sodium chloride did not affect degradation. Most of the non-cross-linked gelatin molecules and their adherent β -tricalcium phosphate particles were dissolved and released in the first day of soaking. The curves revealed a low rate of degradation after four days of soaking, even after the scaffolds had been soaked in deionized water

1
2
3
4 for 42 days. The percent weight remaining declined to 92% at 42 days.
5
6
7
8

9 10 **3.6. Effects of GTP scaffold extracts on rat BMSCs**

11 MTT assay is an important method for evaluating scaffold cytotoxicity. Figure 3 shows
12 the relationship between the number of cells and the soaking period when the GTP
13 scaffold extracts with salt/composite weight ratio of 4:1 were cultured with rat BMSCs
14 for 2 days. The extracts had significantly more cells than the control group ($p < 0.05$).
15 This represents that the GTP scaffold should not be cytotoxic to cells. Moreover, the
16 number of cells increased significantly from day 1 (3.17×10^4) to day 14 (4.42×10^4) of
17 cultivation ($p < 0.05$) and remained almost constant until the end of the 42 day ($4.57 \times$
18 10^4) cultivation period ($p > 0.05$). After 14 days of cultivation, the number of cells had
19 risen to approximately eight times the initial number of cells. These findings suggest
20 that the GTP scaffold extract could promote the proliferation of cells *in vitro*.
21
22
23
24
25
26
27
28
29
30
31
32
33
34
35
36
37

38 **3.7. Rat BMSCs dynamically cultured with the GTP scaffold**

39 A dynamic culture system was employed to improve nutrient supply and metabolite
40 removal. It can provide a mechanical stimulus to the cells. Since the MTT assay
41 revealed that the number of cells remained almost constant after two weeks of culture,
42 the period of dynamic culture was two weeks herein. Figure 4 presents the morphology
43 of rat cells that were dynamically cultured on the GTP scaffold with salt/composite
44 weight ratio of 4:1. An SEM cross-sectional investigation after two weeks of cultivation
45 in osteogenic medium revealed that cells can penetrate the open pores and attach
46 reliably to the walls of the pores in the scaffold. Following dynamic culture, the porous
47 GTP scaffolds with cells were adopted in a follow-up animal study.
48
49
50
51
52
53
54
55
56
57
58
59
60

3.8. Biological response of rat calvarial bone

3.8.1. Gross examination

All animals survived throughout the experiment. The surgical incisions that had been made on the calvarial bone of the rats healed rapidly without evidence of wound infection, scalp effusion, hematoma, festers or other complications. The GTP scaffold was intimately incorporated into the surrounding host bone. No abscess or inflammation of the peripheral osseous tissues at the implantation site was observed, revealing that the implantation of the GTP scaffold in the calvarial bone defect did not cause histopathology or exhibit malbiocompatibility with the peripheral osseous tissues. Moreover, the brain tissues under the GTP scaffold did not exhibit any evidence of cortical inflammation, necrosis or scar formation. The results indicated that the GTP scaffold did not cytotoxically influence the underlying brain tissues.

3.8.2. SEM examination

SEM was employed to visualize the formation of vascularization. Vascularization is essential to the performance of a tissue engineered bone. SEM micrographs in Figure 5A indicate that numerous erythrocytes were present in the scaffold at week 4. This result demonstrated that the porous GTP scaffold induced an angiogenic response in the host tissue, which resulted in vascularization of the implant. Additionally, several osteoblasts had grown to form a layer of cells in the pores of the scaffold, revealing that the scaffold exhibited good cellular affinity and good cytocompatibility (Figure 5B).

3.8.3. Radiographic analysis

Figure 6 presents X-ray photographs of 7 mm skull defects of rats 8 weeks following

1
2
3
4 the application of acellular and cellular GTP scaffolds. Bone was newly formed in the
5 periphery of all porous GTP scaffolds. However, the area of newly regenerated bone
6
7 using the BMSCs-seeded GTP scaffold exceeded that formed using only the porous
8
9 GTP scaffold.
10
11
12

13 14 15 16 **3.8.4. Histological examination** 17

18 Finally, a histological evaluation was conducted to characterize the osteogenic capacity
19 of the BMSCs-seeded GTP scaffold. Following harvest, the scaffold was stained with
20 H&E. Figure 7 displays the histological cross-sections of rat skull defects eight weeks
21 after the application of a BMSCs-seeded GTP scaffold with two weeks of dynamic
22 culture. As shown in the full cross-section of the scaffold (Figure 7A), new bone
23 formation was observed at the periphery of the scaffold. Bone-like tissue was also
24 observed in the interior part of the GTP scaffold, replacing a significant proportion of it
25 (Figures 7A, B). This result revealed that the seeded BMSCs promoted the formation of
26 bone within the scaffold. To verify further the formation of new bone, ALP staining and
27 von Kossa staining were utilized to identify the bone-forming activity and the areas of
28 mineral deposition. ALP staining revealed strong ALP activity, suggestive of possible
29 osteogenic differentiation (Figure 7D). Strongly positive von Kossa staining indicated
30 strong mineralization of the newly formed bone (Figure 7E). These results are similar to
31 that of H&E staining (Figure 7C).
32
33
34
35
36
37
38
39
40
41
42
43
44
45
46
47
48
49
50
51
52
53
54
55
56
57
58
59
60

4. Discussion

An ideal scaffold for application in bone tissue engineering should provide support for cell adhesion, proliferation and differentiation. Gelatin has been identified as a substrate for cell adhesion and proliferation. β -tricalcium phosphates are commonly employed because of their ability to osteoconduct cells into the scaffold. However, β -tricalcium phosphates have such disadvantages as brittleness and low plasticity. A combination of β -tricalcium phosphates with gelatin can overcome these disadvantages. Additionally, the incorporation of β -tricalcium phosphates yields an osteogenic property (Takahashi et al., 2005). The present authors previously developed a novel bone substitute composed of OPCs cross-linked gelatin and β -tricalcium phosphates (GTP composite). The substances released from the GTP composite facilitated the proliferation of MG-63 cells. Moreover, adding OPCs can reduce significantly the rate of degradation of the composite. However, the GTP composite has a denser structure after the addition of OPCs. A scaffold with a porous morphology could especially promote sufficient nutrient supply and effective cell in-growth.

Salt leaching is a very simple approach for producing a porous structure. Salts can exist as solid particles in aqueous media when the salt concentration is above the saturation concentration. Gross *et al.* (2004) revealed that a larger pore volume could be obtained using larger salt particles. Lee *et al.* (2005) used sodium chloride particles of size 300-500 μm to prepare gelatin scaffold with an interconnected macropores structure (average pore size = 350 μm). Therefore, in this study, GTP scaffolds with macroporous morphologies were prepared by chemically cross-linking gelatin/ β -tricalcium phosphate mixtures with OPCs in the presence of various amounts of sodium chloride particles with a size of 420-590 μm . The amount of added salt strongly influenced the

1
2
3
4 morphology of the GTP scaffold. The scaffold formed herein with the salt/composite
5 weight ratio at 4:1 had a relatively homogeneous pore structure and higher porosity. The
6 pore size was 400-550 μm , which was consistent with the original size of the sodium
7 chloride particles. Since the growth of osteoblasts depends on their contact with other
8 cells, the pore size in the scaffold should be more than three times ($>100 \mu\text{m}$) that of the
9 osteoblasts ($\sim 30 \mu\text{m}$) (Köse *et al.*, 2003). Pore size of 200-900 μm was reportedly
10 required for bone tissue engineering (Karageorgiou *et al.*, 2005; Yang *et al.*, 2001). de
11 Groot (1980) demonstrated that the optimal pore size for the in-growth of bone was
12 approximately 200-500 μm . Sous *et al.* (1998) claimed that bone substitutes with
13 macropore diameters within the 100-800 μm range can facilitate connections with
14 connective tissue and promote bone in-growth. Moreover, the interconnected pores
15 provide tunnels that carry nutrients and waste to and from cells. Accordingly, high
16 porosity ($\sim 73\%$), large pores and a three-dimensionally interconnected pore structure in
17 the GTP scaffold with salt/composite weight ratio of 4:1 provide a large surface area for
18 the attachment of cells and space for the in-growth of bone tissue following
19 implantation.
20
21
22
23
24
25
26
27
28
29
30
31
32
33
34
35
36
37
38
39
40
41

42 In this investigation, a rapid mass loss of the GTP scaffolds of approximately 4 wt%
43 occurred within the first day of soaking in deionized water. The degradation process
44 became slow from then until day 42. The authors' earlier study found that the
45 incorporation of 5–10 wt% OPCs into gelatin-based composites markedly reduced their
46 rate of degradation (Chen *et al.*, 2008). The *in vitro* degradations of GTP scaffolds
47 treated with various amounts of salt were similar. This behavior may be attributable to
48 the scaffolds having the same extent of cross-linking. However, the porosity of the
49 scaffold affected the swelling rate. A scaffold with higher porosity had a higher water
50
51
52
53
54
55
56
57
58
59
60

1
2
3
4 adsorption capacity because of the increase of voids to capillary-adsorbed water.

5
6
7 In the authors' previous study, the gelatin molecules and calcium ions gradually
8
9 released from the GTP composite could facilitate the growth of MG-63 cells *in vitro*.
10
11 Additionally, the incorporation of OPCs into gelatin-based composites was
12
13 advantageous not only in terms of increasing scaffold stability but also in facilitating the
14
15 proliferation of MG-63 cells. In this study, an approximately eight-fold increase in the
16
17 number of cells was detected after 14 days of cultivation in GTP scaffold extracts. The
18
19 high proliferation rate of cells in the GTP scaffold extracts was attributable to the
20
21 release of gelatin, OPCs and calcium ions.
22
23
24

25
26 The *in vivo* bone-regenerative capacity of the porous GTP scaffold was investigated
27
28 in a rat calvarial defect model. The cranial site is of particular interest, because several
29
30 bone graft substitute materials have been employed clinically in craniomaxillofacial
31
32 applications (Holmes and Hagler, 1998). In the rat cranium, a circular bone defect of
33
34 7-mm diameter is a critical-sized defect (Canter *et al.*, 2010; Koh *et al.*, 2008; Ueno *et*
35
36 *al.*, 2007). This critical-size defect can heal spontaneously only by the invasion of soft
37
38 tissue and not by bony bridging (Ueno *et al.*, 2007). Such defects are therefore good
39
40 delayed-healing models (Schmitz and Hollinger, 1986). Since the GTP scaffold is highly
41
42 malleable, it can be perfectly molded into the calvarial bone defect without fracture,
43
44 remaining in place throughout the post-operative period. At four weeks postoperatively,
45
46 gross examinations revealed that the GTP scaffold was both biocompatible and
47
48 biodegradable. As it degraded, some of its components were released into the defect.
49
50 They included gelatin molecules, calcium and phosphorous ions. These were nutrients
51
52 for new bone generation.
53
54
55
56
57

58
59 The brain tissues under the GTP scaffold did not exhibit any cortical inflammation or
60

1
2
3
4 scar formation. These results are consistent with those of the authors' previous studies.
5
6
7 The unchained OPCs released from the GTP scaffold did not harm the surrounding bone
8
9 tissue (Chen *et al.*, 2008; Chen *et al.*, 2009).
10

11 SEM examination revealed that numerous erythrocytes were present in the
12
13 BMSCs-seeded scaffold at week four, indicating that blood vessels from the
14
15 neighboring host tissues had successfully invaded the scaffold. The SEM image shows
16
17 numerous cells around the pores in the BMSCs-seeded GTP scaffold after four weeks of
18
19 post-implantation, indicating that the macroporous surface of the implanted scaffold
20
21 could provide a suitable environment for cell attachment *in vivo*. Additionally, the
22
23 release of gelatin and calcium from the GTP scaffold promoted the proliferation of cells
24
25 *in vitro*. These results demonstrated that the seeded BMSCs, post-implant
26
27 vascularization and the release of nutritious elements from the scaffold were possible
28
29 causes of the proliferation of the cells at the bone defect at the fourth week
30
31 post-implantation. These regenerating cells could modulate further development of bone
32
33 tissue.
34
35
36
37
38
39

40 Radiographic and histological analyses verified the growth of new bone into the
41
42 calvarial defects treated with the GTP scaffold after eight weeks of implantation. A
43
44 porous GTP scaffold combined with BMSCs promoted bone growth in the defect site
45
46 beyond that achieved using an acellular scaffold. Moreover, the examination of the
47
48 H&E-stained sections of the craniectomy sites revealed that bone-like tissue replaced a
49
50 significant amount of the GTP scaffold, suggesting that the use of seeded BMSCs could
51
52 result in bone in-growth within the GTP scaffold. Several studies have found that the
53
54 presence of mesenchymal stem cells in a bone substitute can enhance bone formation.
55
56
57
58 For instance, Bruder *et al.* (1998b) loaded autologous BMSCs onto porous ceramic
59
60

1
2
3
4 scaffolds and implanted them into dog femoral defects. They demonstrated that the
5 amount of new bone in the BMSCs-loaded implants significantly exceeded that in the
6
7 cell-free implants. Kon *et al.* (2000) suggested that the use of autologous BMSCs in
8
9 conjunction with porous hydroxyapatite ceramic-based carriers resulted in faster bone
10
11 repair in a sheep model than was achieved using hydroxyapatite ceramic alone. van den
12
13 Dolder *et al.* (2003) used a combination of titanium fiber mesh and rat BMSCs to
14
15 reconstruct cranial defects in rats and found that the use of cell-loaded implants was
16
17 associated with filling with significantly more bone than was the use of non-cell-loaded
18
19 meshes. Mankani *et al.* (2006) reconstructed canine cranial using autologous
20
21 BMSCs-containing hydroxyapatite/tricalcium phosphate and found that a
22
23 BMSCs-containing transplant formed significantly more bone than a BMSCs-free
24
25 transplant. Yoshii *et al.* (2009) identified new bone formation in most fresh autologous
26
27 bone marrow-seeded porous β -tricalcium phosphates; however, they detected no bone
28
29 formation in β -tricalcium phosphates unless bone marrow was introduced. Similarly,
30
31 Zhang *et al.* (2010) used fetal mesenchymal stem cells that were loaded onto
32
33 macroporous poly- ϵ -caprolactone/tricalcium phosphate scaffolds and
34
35 dynamically-cultured for two weeks. They found that cell-seeded scaffolds yielded more
36
37 vascularization and bone formation than acellular scaffolds in rat femoral defects. The
38
39 cited studies indicated that the use of mesenchymal stem cells combined with scaffolds
40
41 can improve the bone healing capacity of scaffolds, probably by reducing the time for
42
43 the cells to invade the defect site.
44
45
46
47
48
49
50
51
52
53
54
55
56
57
58
59
60

5. Conclusions

Porous biodegradable GTP scaffolds with pores of size 400-550 μm were successfully fabricated using a salt-leaching method. *In vitro* assay demonstrated that the cells could penetrate the pores. The BMSCs-seeded GTP scaffold was used to fill a bone defect in the rat calvarial model and successfully promoted bone regeneration. Accordingly, the combination of the porous GTP scaffold with BMSCs has promise for application in bone tissue engineering.

Acknowledgments

The authors would like to thank the National Science Council of the Republic of China, Taiwan (contract No. NSC96-2628-E-166-008-MY3) and the China Medical University (contract No. CMU98-S-48) for financially supporting this research.

References

- Bernhardt A, Despong F, Lode A. *et al.* 2009; Proliferation and osteogenic differentiation of human bone marrow stromal cells on alginate-gelatin-hydroxyapatite scaffolds with anisotropic pore structure. *J Tissue Eng Regen Med* **3**: 54-62.
- Bigi A, Bracci B, Panzavolta S. 2004; Effect of added gelatin on the properties of calcium phosphate cement. *Biomaterials* **25**: 2893-2899.
- Bruder SP, Jaiswal N, Ricalton NS, *et al.* 1998a; Mesenchymal stem cells in osteobiology and applied bone regeneration. *Clin Orthop Rel Res* **355**: S247-S256.
- Bruder SP, Kraus KH, Goldberg VM, *et al.* 1998b; The effect of implants loaded with autologous mesenchymal stem cells on the healing of canine segmental bone defects. *J Bone Joint Surg Am* **80**: 985-996.
- Canter HI, Vargel I, Korkusuz P, *et al.* 2010; Effect of use of slow release of bone morphogenetic protein-2 and transforming growth factor-beta-2 in a chitosan gel matrix on cranial bone graft survival in experimental cranial critical size defect model. *Ann Plast Surg* **64**: 342-350.
- Chen KY, Shyu PC, Chen YS, *et al.* 2008; Novel bone substitute composed of oligomeric proanthocyanidins-crosslinked gelatin and tricalcium phosphate. *Macro Biosci* **8**: 942-950.
- Chen KY, Shyu PC, Dong GC, *et al.* 2009; Reconstruction of calvarial defect using a tricalcium phosphate-oligomeric proanthocyanidins cross-linked gelatin composite. *Biomaterials* **30**: 1682-1688.
- de Groot K. 1980; Bioceramics consisting of calcium phosphate salts. *Biomaterials* **1**: 47-50.
- Gross KA, Rodríguez-Lorenzo LM. 2004; Biodegradable composite scaffolds with an interconnected spherical network for bone tissue engineering. *Biomaterials* **25**: 4955-4962.
- Han B, Jaurequi J, Tang BW, *et al.* 2003; Proanthocyanidin: a natural crosslinking reagent for stabilizing collagen matrices. *J Biomed Mater Res A* **65**: 118-124.
- Holmes RE, Hagler HK. 1988; Porous hydroxyapatite as a bone graft substitute in cranial reconstruction: a histometric study. *Plast Reconstr Surg* **81**: 662-671.
- Karageorgiou V, Kaplan D. 2005; Porosity of 3D biomaterial scaffolds and osteogenesis.

- 1
2
3
4
5 *Biomaterials* **26**: 5474-5491.
- 6
7 Kim HW, Kim HE, Salih V. 2005a; Stimulation of osteoblast responses to biomimetic
8 nanocomposites of gelatin-hydroxyapatite for tissue engineering scaffolds.
9 *Biomaterials* **26**: 5221-5230.
- 10
11 Kim S, Nimni ME, Yang Z, *et al.* 2005b; Chitosan/gelatin-based films crosslinked by
12 proanthocyanidin. *J Biomed Mater Res B* **75**: 442-450.
- 13
14 Kim H, Suh H, Jo SA, *et al.* 2005c; *In vivo* bone formation by human marrow stromal
15 cells in biodegradable scaffolds that release dexamethasone and ascorbate-
16 2-phosphate. *Biochem Biophys Res Commun* **332**: 1053-1060.
- 17
18 Koh JT, Zhao Z, Wang Z, *et al.* 2008; Combinatorial gene therapy with BMP2/7
19 enhances cranial bone regeneration. *J Dent Res* **87**: 845-849.
- 20
21 Kon E, Muraglia A, Corsi A, *et al.* 2000; Autologous bone marrow stromal cells loaded
22 onto porous hydroxyapatite ceramic accelerate bone repair in critical-size defects of
23 sheep long bones. *J Biomed Mater Res A* **49**: 328-337.
- 24
25 Köse GT, Kenar H, Hasirci N, *et al.* 2003; Macroporous poly(3-hydroxybutyrate-co-3-
26 hydroxyvalerate) matrices for bone tissue engineering. *Biomaterials* **24**: 1949-1958.
- 27
28 Lee SB, Kim YH, Chong MS, *et al.* 2005; Study of gelatin-containing artificial skin V:
29 Fabrication of gelatin scaffolds using a salt-leaching method. *Biomaterials* **26**:
30 1961-1968.
- 31
32 Liu BS, Yao CH, Chen YS, *et al.* 2003; *In vitro* evaluation of degradation and
33 cytotoxicity of a novel composite as a bone substitute. *J Biomed Mater Res A* **67**:
34 1163-1169.
- 35
36 Lin FH, Yao CH, Sung JS, *et al.* 1998; Biological effects and cytotoxicity of the
37 composite composed by tricalcium phosphate and glutaraldehyde cross-linked gelatin.
38 *Biomaterials* **19**: 905-917.
- 39
40 Mankani MH, Kuznetsov SA, Shannon B, *et al.* 2006; Canine cranial reconstruction
41 using autologous bone marrow stromal cells. *Am J Pathol* **168**: 542-550.
- 42
43 Ogose A, Kondo N, Umezu H, *et al.* 2006; Histological assessment in grafts of highly
44 purified beta-tricalcium phosphate (OSferion®) in human bones. *Biomaterials* **27**:
45 1542-1549.
- 46
47 Schmitz JP, Hollinger JO. 1986; The critical size defect as an experimental model for
48 craniomandibulofacial nonunions. *Clin Orthop Relat Res* **205**:299-308.
- 49
50 Sous M, Bareille R, Rouais F, *et al.* 1998; Cellular biocompatibility and resistance to
51
52
53
54
55
56
57
58
59
60

- 1
2
3
4
5 compression of macroporous β -tricalcium phosphate ceramics. *Biomaterials* **19**:
6 2147-2153.
7
- 8 Sung HW, Huang DM, Chang WH, *et al.* 1999; Evaluation of gelatin hydrogel
9 crosslinked with various crosslinking agents as bioadhesives: *in vitro* study. *J Biomed*
10 *Mater Res* **46**: 520-530.
11
- 12 Tabata Y, Hong L, Miyamoto S, *et al.* 2000; Bone formation at a rabbit skull defect by
13 autologous bone marrow cells combined with gelatin microspheres containing
14 TGF- β 1. *J Biomater Sci Polymer Edn* **11**: 891-901.
15
- 16 Takahashi Y, Yamamoto M, Tabata Y. 2005; Osteogenic differentiation of mesenchymal
17 stem cells in biodegradable sponges composed of gelatin and β -tricalcium phosphate.
18 *Biomaterials* **26**: 3587-3596.
19
- 20 Ueno T, Sakata Y, Hirata A, *et al.* 2007; The evaluation of bone formation of the
21 whole-tissue periosteum transplantation in combination with β -tricalcium phosphate
22 (TCP). *Ann Plast Surg* **59**: 707-712.
23
- 24 Van den Dolder J, Farber E, Spauwen PHM, *et al.* 2003; Bone tissue reconstruction
25 using titanium fiber mesh combined with rat bone marrow stromal cells. *Biomaterials*
26 **24**: 1745-1750.
27
- 28 Vrouwenvelder WCA, Groot CG, de Groot K. 1992; Behaviour of fetal rat osteoblasts
29 cultured *in vitro* on bioactive glass and nonreactive glasses. *Biomaterials* **13**:
30 382-392.
31
- 32 Yang S, Leong KF, Du Z, *et al.* 2001; The design of scaffolds for use in tissue
33 engineering: part I. traditional factors. *Tissue Eng* **7**: 679-689.
34
- 35 Yoshii T, Sotome S, Torigoe I, *et al.* 2009; Fresh bone marrow introduction into porous
36 scaffolds using a simple low-pressure loading method for effective osteogenesis in a
37 rabbit model. *J Orthop Res* **27**: 1-7.
38
- 39 Zhai W, Chang J, Lin K, *et al.* 2006; Crosslinking of decellularized porcine heart valve
40 matrix by procyanidins. *Biomaterials* **27**: 3684-3690.
41
- 42 Zhang Z-Y, Teoh S-H, Chong MSK, *et al.* 2010; Neo-vascularization and bone
43 formation mediated by fetal mesenchymal stem cell tissue-engineered bone grafts in
44 critical-size femoral defects. *Biomaterials* **31**: 608-620.
45
- 46 Zhao F, Grayson WL, Ma T, *et al.* 2006; Effects of hydroxyapatite in 3-D
47 chitosan-gelatin polymer network on human mesenchymal stem cell construct
48 development. *Biomaterials* **27**: 1859-1867.
49
50
51
52
53
54
55
56
57
58
59
60

1
2
3
4
5
6
7
8
9
10
11
12
13
14
15
16
17
18
19
20
21
22
23
24
25
26
27
28
29
30
31
32
33
34
35
36
37
38
39
40
41
42
43
44
45
46
47
48
49
50
51
52
53
54
55
56
57
58
59
60

For Peer Review

Figure captions

Figure 1. SEM images of the cross-section morphologies of the GTP scaffolds with salt/composite weight ratios of (A) 3:1, (B) 4:1 and (C) 5:1

Figure 2. Effects of salt/composite weight ratio on the (A) swelling ratio and (B) weight loss of the GTP scaffolds

Figure 3. Effect of the GTP scaffold soaking solutions on the cell number after culturing for 2 days

Figure 4. SEM picture of cells attaching and adhering to the pore walls of the GTP scaffold with salt/composite weight ratio of 4:1 after dynamically culturing for 2 weeks

Figure 5. SEM observation of erythrocytes (A) and osteoblasts (B) regenerating around the pores of BMSCs-seeded GTP scaffold after 4 weeks of post-implantation

Figure 6. Radiographs of rat calvarial bone-covered implants removed after (A) porous GTP scaffold alone and (B) cells-seeded GTP scaffold with 2 week of dynamic culture were implanted into the calvarial bone defects for 8 weeks (HB = host bone, NB = new bone, dotted line indicates the original margin of the calvarial bone defect). The dotted circles indicate the original defect

Figure 7. Histological image of H&E-stained BMSCs-seeded GTP scaffold with 2 weeks of dynamic culture implanted in calvarial defects for 8 weeks (A). Enlarged view of central part is shown in (B). Enlarged views of peripheral part are shown in (C-E). (BLT = bone-like tissue, HB = host bone, NB = new bone)

1
2
3
4
5
6
7
8
9
10
11
12
13
14
15
16
17
18
19
20
21
22
23
24
25
26
27
28
29
30
31
32
33
34
35
36
37
38
39
40
41
42
43
44
45
46
47
48
49
50
51
52
53
54
55
56
57
58
59
60

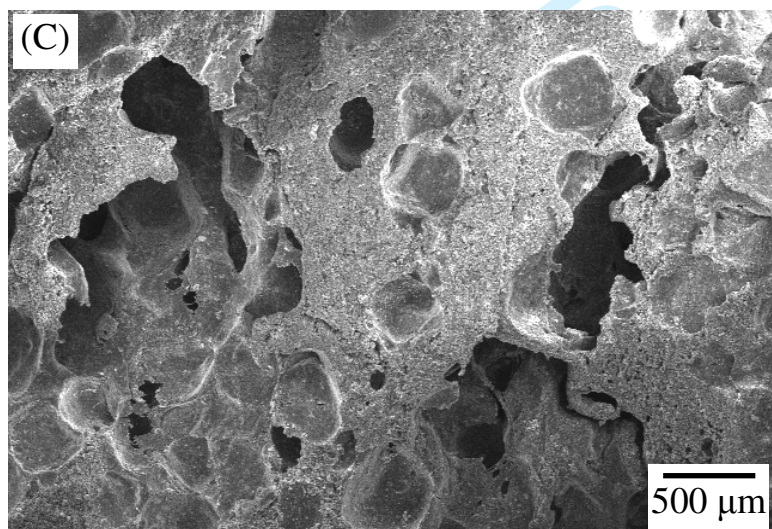
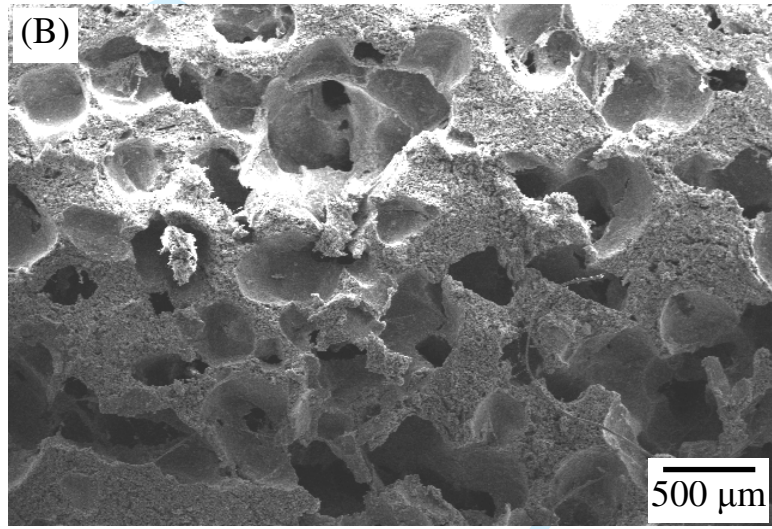
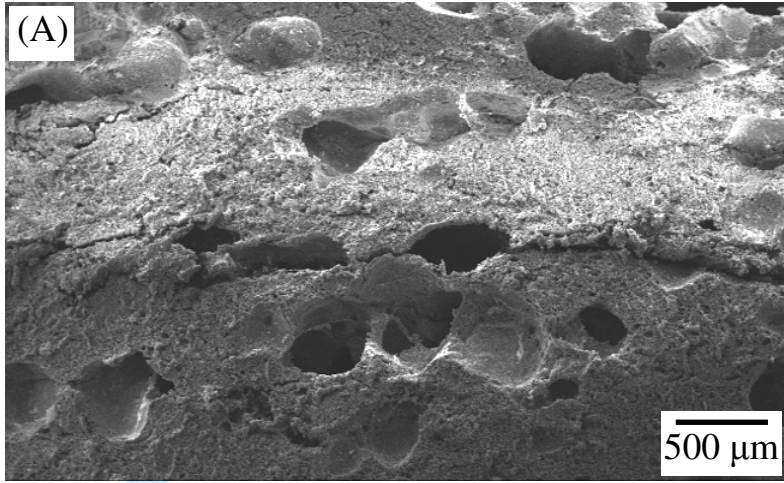


Figure 1

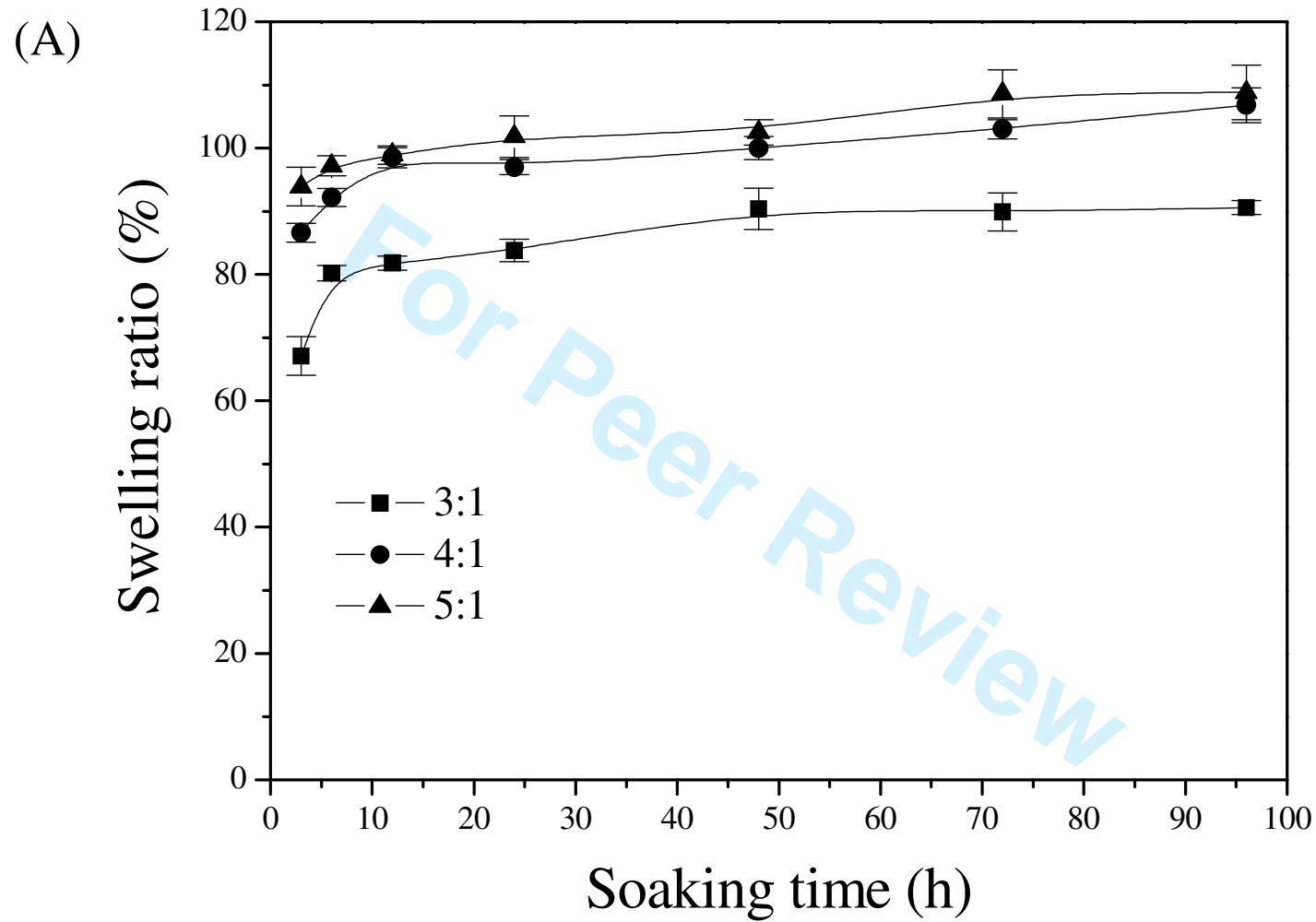


Figure 2A

(B)

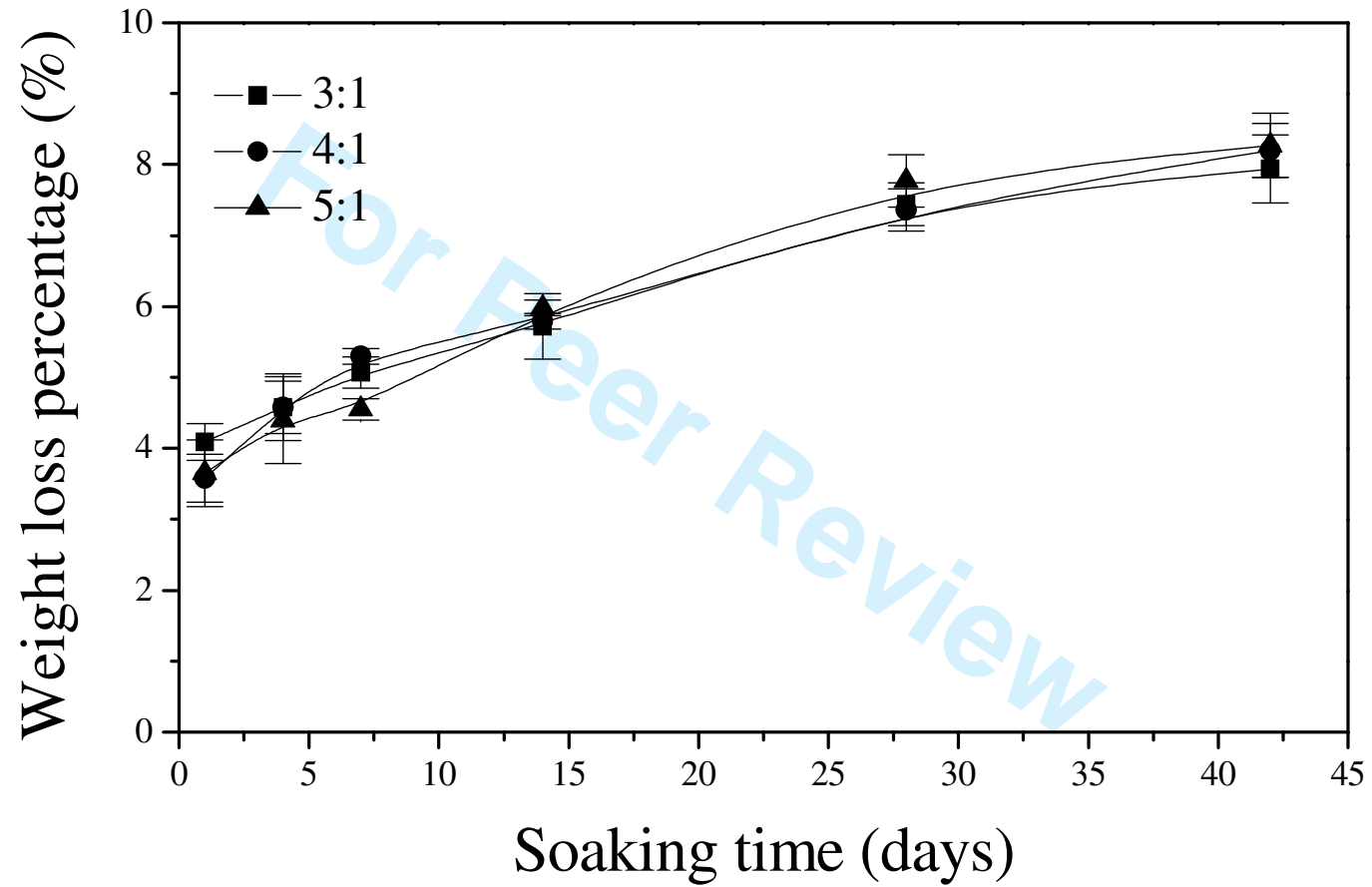


Figure 2B

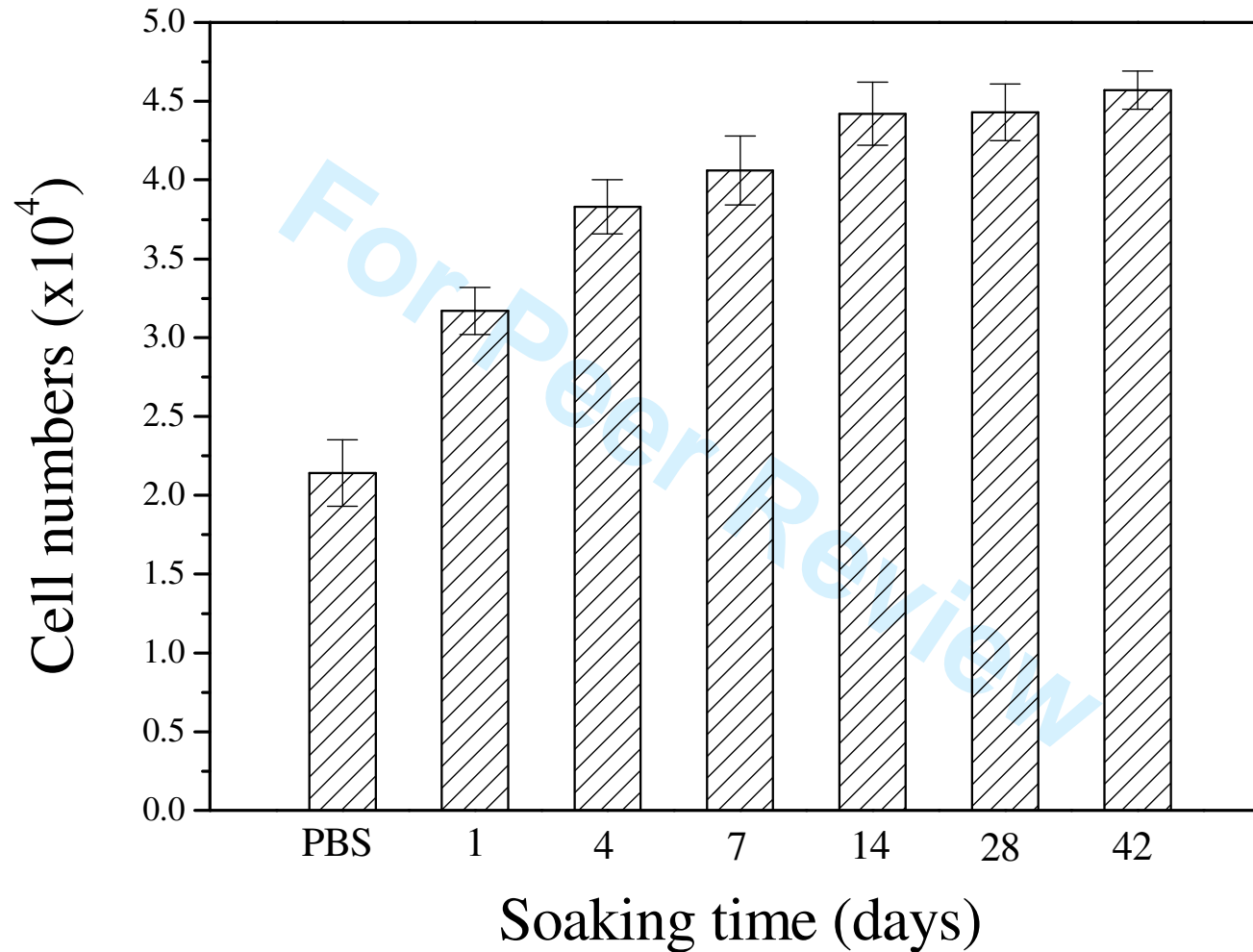


Figure 3

1
2
3
4
5
6
7
8
9
10
11
12
13
14
15
16
17
18
19
20
21
22
23
24
25
26
27
28
29
30
31
32
33
34
35
36
37
38
39
40
41
42
43
44
45
46
47
48
49
50
51
52
53
54
55
56
57
58
59
60

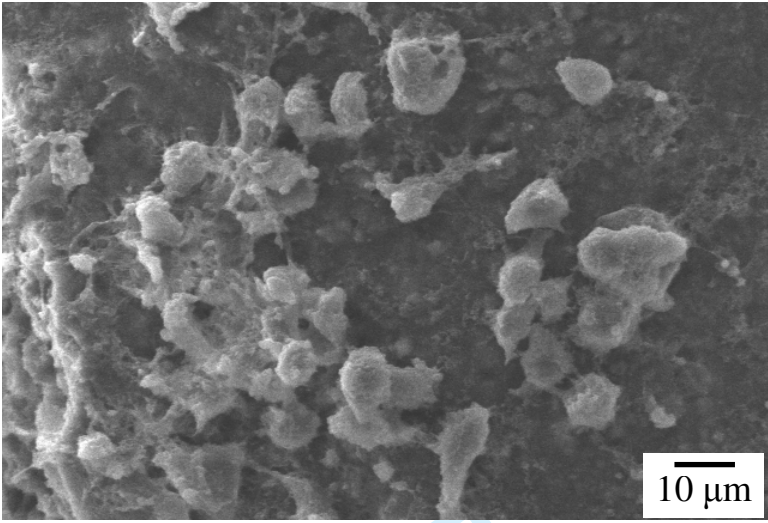


Figure 4

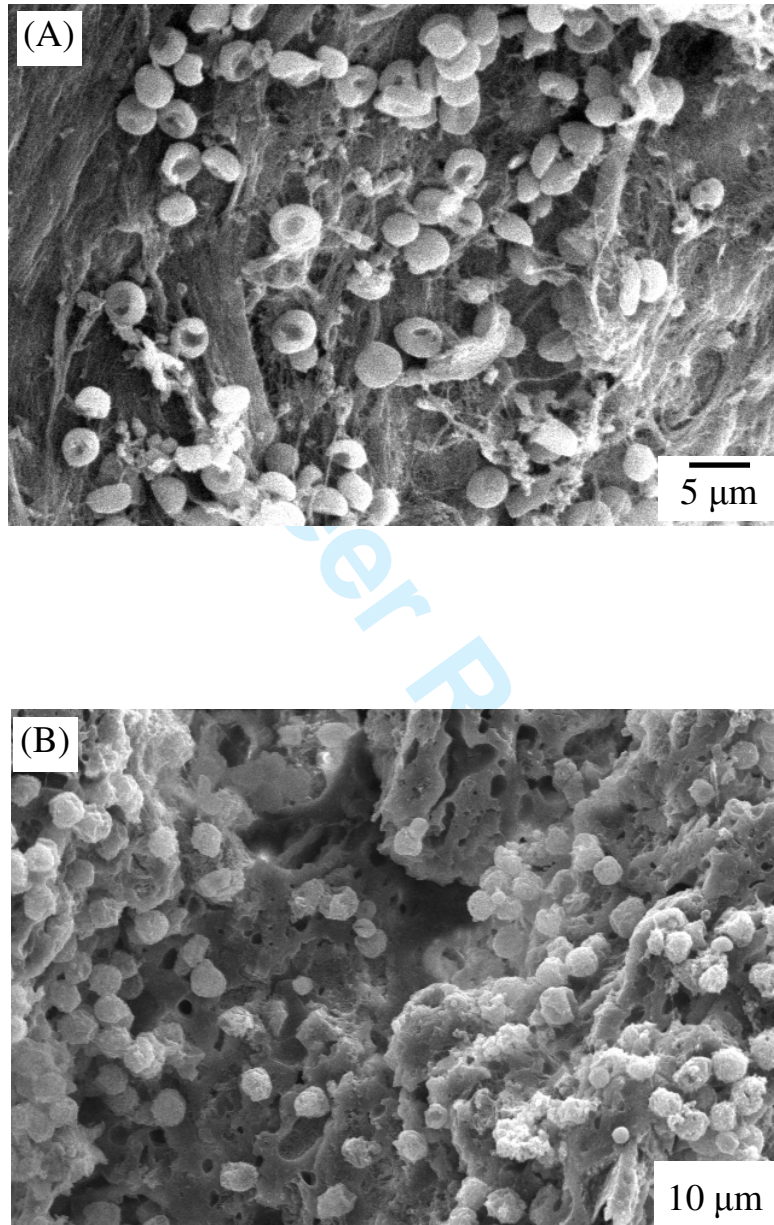


Figure 5

1
2
3
4
5
6
7
8
9
10
11
12
13
14
15
16
17
18
19
20
21
22
23
24
25
26
27
28
29
30
31
32
33
34
35
36
37
38
39
40
41
42
43
44
45
46
47
48
49
50
51
52
53
54
55
56
57
58
59
60

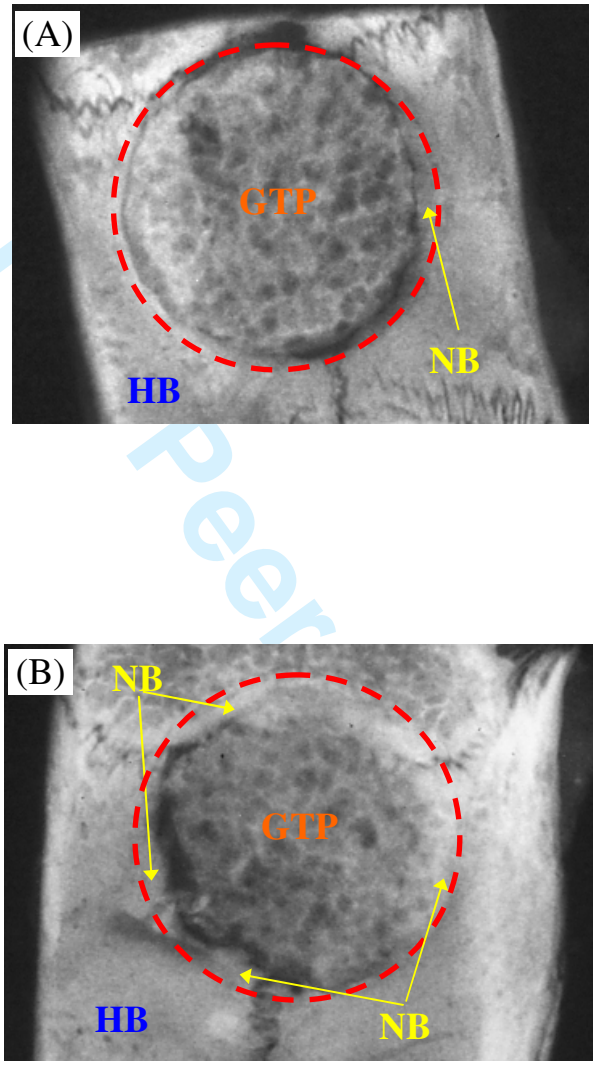
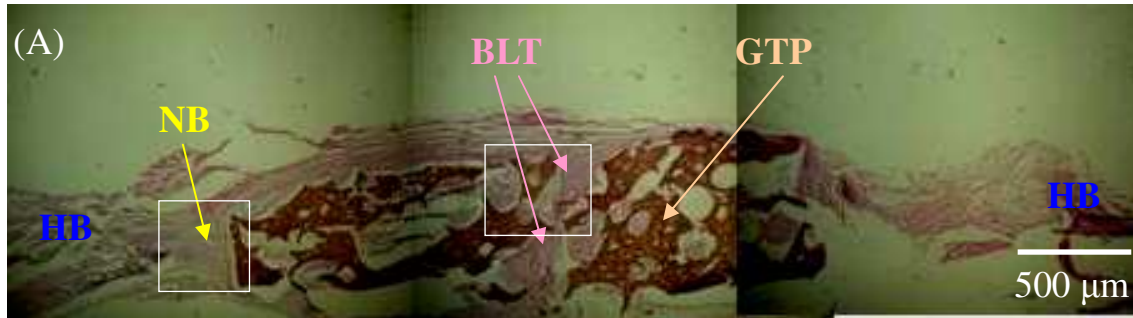
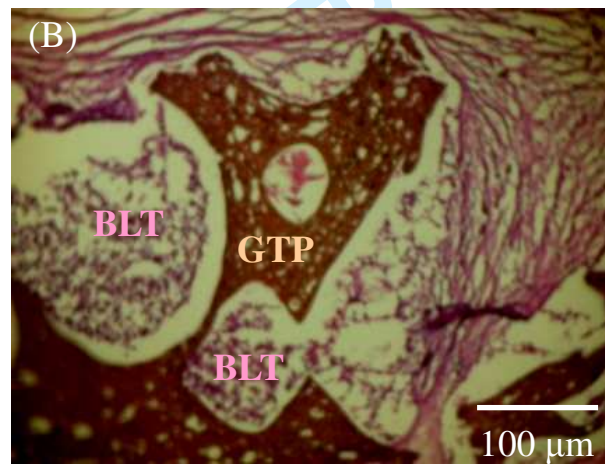


Figure 6



H&E stain



1
2
3
4
5
6
7
8
9
10
11
12
13
14
15
16
17
18
19
20
21
22
23
24
25
26
27
28
29
30
31
32
33
34
35
36
37
38
39
40
41
42
43
44
45
46
47
48
49
50
51
52
53
54
55
56
57
58
59
60

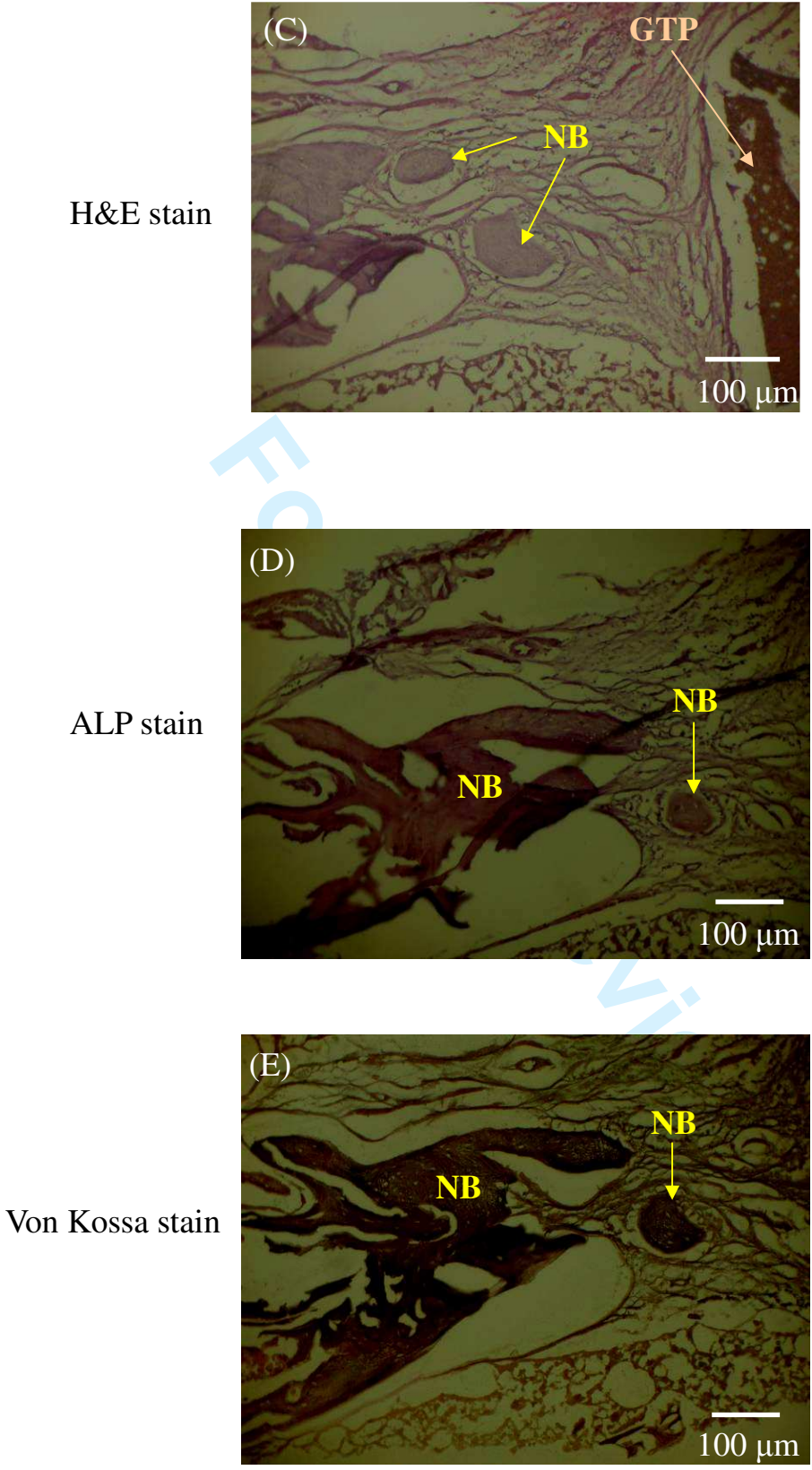


Figure 7